Genotype-phenotype correlation at codon 1740 ofSETD2

Rabin, Rachel; Radmanesh, Alireza; Glass, Ian A.; Dobyns, William B.; Aldinger, Kimberly A.; Shieh, Joseph T.; Romoser, Shelby; Bombei, Hannah; Dowsett, Leah; Trapane, Pamela

Published in:
American Journal of Medical Genetics. Part A

DOI:
10.1002/ajmg.a.61724

Publication date:
2020

Received: 24 October 2019 | Revised: 10 March 2020 | Accepted: 8 May 2020

DOI: 10.1002/ajmg.a.61724

ORIGINAL ARTICLE

AMERICAN JOURNAL OF medical genetics PART A WILEY

Genotype–phenotype correlation at codon 1740 of *SETD2*

Rachel Rabin[1] | Alireza Radmanesh[2] | Ian A. Glass[3,4] | William B. Dobyns[3,4,5] | Kimberly A. Aldinger[3] | Joseph T. Shieh[6] | Shelby Romoser[7] | Hannah Bombei[7] | Leah Dowsett[8] | Pamela Trapane[9] | John A. Bernat[7] | Janice Baker[10] | Nancy J. Mendelsohn[10] | Bernt Popp[11] | Manuela Siekmeyer[12] | Ina Sorge[13] | Francis Hugh Sansbury[14] | Patrick Watts[15] | Nicola C. Foulds[16] | Jennifer Burton[17] | George Hoganson[17] | Jane A. Hurst[18] | Lara Menzies[18] | Deborah Osio[19] | Larissa Kerecuk[20] | Jan M. Cobben[21,22] | Khadijé Jizi[23] | Sebastien Jacquemont[24,25] | Stacey A. Bélanger[26,27] | Katharina Löhner[28] | Hermine E. Veenstra-Knol[28] | Henny H. Lemmink[28] | Jennifer Keller-Ramey[29] | Ingrid M. Wentzensen[29] | Sumit Punj[29] | Kirsty McWalter[29] | Jerica Lenberg[30] | Katarzyna A. Ellsworth[30] | Kelly Radtke[31] | Schahram Akbarian[32] | John Pappas[1,33]

[1]Clinical Genetic Services, Department of Pediatrics, NYU School of Medicine, New York, New York

[2]Division of Pediatric Neuroradiology, Department of Radiology, NYU School of Medicine, New York, New York

[3]Center for Integrative Brain Research, Seattle Children's Research Institute, Seattle, Washington

[4]Department of Pediatrics, Division of Medical Genetics, University of Washington, Seattle, Washington

[5]Department of Neurology, University of Washington, Seattle, Washington

[6]Institute for Human Genetics, Division of Medical Genetics, Department of Pediatrics, Benioff Children's Hospital, University of California San Francisco, San Francisco, California

[7]Division of Medical Genetics and Genomics, Stead Family Department of Pediatrics, University of Iowa Hospitals, Iowa City, Iowa

[8]Kapi'olani Medical Specialists and Department of Pediatrics, University of Hawai'i John A. Burns School of Medicine, Honolulu, Hawaii

[9]Division of Pediatric Genetics, Department of Pediatrics, University of Florida College of Medicine-Jacksonville, Jacksonville, Florida

[10]Genomic Medicine, Children's Minnesota, Minneapolis, Minnesota

[11]Institute of Human Genetics, University of Leipzig Hospitals and Clinics, Leipzig, Germany

[12]Department of Pediatrics Hospital for Children and Adolescents, University of Leipzig Hospitals and Clinics, Leipzig, Germany

[13]Department of Pediatric Radiology, University of Leipzig Hospitals and Clinics, Leipzig, Germany

[14]All Wales Medical Genomics Service, Institute of Medical Genetics, Cardiff and Vale University Health Board, University Hospital of Wales, Cardiff, UK

[15]Department of Ophthalmology, Cardiff and Vale University Health Board, University Hospital of Wales, Cardiff, UK

[16]Wessex Clinical Genetics Services, Southampton University Hospital NHS Foundation Trust, Southampton, UK

[17]University of Illinois College of Medicine at Peoria, Peoria, Illinois

[18]Department of Clinical Genetics, Great Ormond Street Hospital, London, UK

[19]Department of Clinical Genetics, Birmingham Women's and Children's NHS Foundation Trust, Birmingham, UK

[20]Renal Department, Birmingham Women's and Children's NHS Foundation Trust, Birmingham, UK

[21]North West Thames Regional Genetic Services, Northwick Park Hospitals NHS Foundation Trust, London, UK

[22]Emma Children Hospital, Amsterdam, The Netherlands

[23]CHU Sainte-Justine Hospital, Montreal, Quebec, Canada

Rachel Rabin and John Pappas equal contribution to this manuscript.

[24]CHU Sainte-Justine Research Centre, Montreal, Quebec, Canada

[25]Department of Pediatrics, University of Montreal, Montreal, Quebec, Canada

[26]Development Clinic, CHU Sainte-Justine Hospital, Montreal, Quebec, Canada

[27]Department of Medicine, University of Montreal, Montreal, Quebec, Canada

[28]Department of Genetics, University of Groningen, University Medical Centre Groningen, Groningen, The Netherlands

[29]GeneDx, Gaithersburg, Maryland

[30]Rady Children's Hospital Institute for Genomic Medicine, San Diego, California

[31]Department of Clinical Diagnostics, Ambry Genetics, Aliso Viejo, California

[32]Friedman Brain Institute and Department of Psychiatry, Icahn School of Medicine at Mount Sinai, New York, New York

[33]Clinical Genetics, NYU Orthopedic Hospital, New York, New York

Correspondence
Rachel Rabin, Clinical Genetic Services, Department of Pediatrics, NYU School of Medicine, 145 E. 32nd St, PH, New York, NY 10016.
Email: rachel.rabin@nyulangone.org

Funding information
Deutsche Forschungsgemeinschaft, Grant/Award Number: PO2366/2-1; National Institute for Health Research; Republic of Ireland REC, Grant/Award Number: GEN/284/12; Cambridge South REC, Grant/Award Number: 10/H0305/83; Department of Health, Grant/Award Number: WT098051; Health Innovation Challenge Fund, Grant/Award Number: HICF-1009-003; Medical Research Council; Cancer Research UK; Wellcome Trust; National Institute for Health Research

Abstract

The SET domain containing 2, histone lysine methyltransferase encoded by *SETD2* is a dual-function methyltransferase for histones and microtubules and plays an important role for transcriptional regulation, genomic stability, and cytoskeletal functions. Specifically, *SETD2* is associated with trimethylation of histone H3 at lysine 36 (H3K36me3) and methylation of α-tubulin at lysine 40. Heterozygous loss of function and missense variants have previously been described with Luscan-Lumish syndrome (LLS), which is characterized by overgrowth, neurodevelopmental features, and absence of overt congenital anomalies. We have identified 15 individuals with de novo variants in codon 1740 of *SETD2* whose features differ from those with LLS. Group 1 consists of 12 individuals with heterozygous variant c.5218C>T p.(Arg1740Trp) and Group 2 consists of 3 individuals with heterozygous variant c.5219G>A p.(Arg1740Gln). The phenotype of Group 1 includes microcephaly, profound intellectual disability, congenital anomalies affecting several organ systems, and similar facial features. Individuals in Group 2 had moderate to severe intellectual disability, low normal head circumference, and absence of additional major congenital anomalies. While LLS is likely due to loss of function of *SETD2*, the clinical features seen in individuals with variants affecting codon 1740 are more severe suggesting an alternative mechanism, such as gain of function, effects on epigenetic regulation, or posttranslational modification of the cytoskeleton. Our report is a prime example of different mutations in the same gene causing diverging phenotypes and the features observed in Group 1 suggest a new clinically recognizable syndrome uniquely associated with the heterozygous variant c.5218C>T p.(Arg1740Trp) in *SETD2*.

KEYWORDS
clinical genetics, genotype phenotype, histone modification, neurodevelopmental, SETD2

1 | INTRODUCTION

The SET domain containing 2, histone lysine methyltransferase (*SETD2*) gene (MIM#612778), codes for a histone methyltransferase mediating tri-methylation of the histone H3-lysine 36 residue (H3K36me3) (Edmunds, Mahadevan, & Clayton, 2008). While the H3K36me3 mark is primarily enriched over the gene bodies of actively transcribed genes, SETD2-regulated H3K36me3 is considered broadly relevant for preventing aberrant transcription arising from cryptic transcription start sites in gene bodies, regulation of RNA splicing, and genomic stability. SETD2 serves as a binding site of DNA mismatch repair and other DNA damage response-associated protein complexes (McDaniel & Strahl, 2017; Zhou, Goren, & Bernstein, 2011). In addition, SETD2 methylates transcription factors such as STAT1, a mechanism of critical importance for antiviral response pathways including interferon signaling (Chen et al., 2017). Furthermore, SETD2 has been implicated in

maintenance of genomic stability through methylation of cytoskeletal alpha-tubulin during mitosis and cytokinesis (Park et al., 2016). In mice, *Setd2* knockouts are embryonic lethal, indicating a key role in development (Hu et al., 2010; Rega et al., 2001).

Variants in *SETD2* were initially identified by research next generation based exome sequencing of parent–child trios diagnosed with sporadic autism spectrum disorder (ASD) through the Simmons simplex collection (SSC) (Iossifov et al., 2014; O'Roak et al., 2012; O'Roak et al., 2012). This research identified three variants in *SETD2*, the paternally inherited p.(Cys94*), the maternally inherited p.(Gln7*), and the de novo p.(Ile41Phe) mutations in children with autism from SSC (O'Roak, Vives, Fu, et al., 2012; O'Roak, Vives, Girirajan, et al., 2012). Since then, *SETD2* variants have been associated with ASD and a specific neurodevelopmental disorder named Luscan-Lumish syndrome (LLS) (Lumish, Wynn, Devinsky, & Chung, 2015; Luscan et al., 2014). To date, there are 10 individuals reported in the literature with variants identified in *SETD2* which have all been observed in children with autistic features and/or LLS. Eight of these patients had truncating variants: six were de novo, two were inherited, and one had unknown inheritance. Two of these patients had de novo missense variants. All the variants are absent from population databases, except for one inherited nonsense variant (Lek et al., 2016). LLS is a Sotos-like syndrome characterized by ASD, normal to moderate intellectual disability with developmental delays, macrocephaly, obesity, advanced bone age, long face and nose with malar hypoplasia, down-slanted palpebral fissures, and prominent mandible with pointed chin (Lumish et al., 2015; Luscan et al., 2014; O'Roak, Vives, Fu, et al., 2012; O'Roak, Vives, Girirajan, et al., 2012; Tlemsani et al., 2016; van Rij et al., 2018).

Here we describe 15 individuals with missense variants in codon 1740 of *SETD2* who present with a specific phenotype different from individuals previously reported with *SETD2* variants. Twelve individuals with heterozygosity of the c.5218C>T p.(Arg1740Trp) variant in *SETD2* (NM_014159.6) present with profound intellectual disability, microcephaly, and multiple congenital anomalies affecting several organ systems. Three individuals with heterozygosity of the c.5219G>A p.(Arg1740Gln) variant in *SETD2* (NM_014159.6) present with moderate to severe intellectual disability, low normal head circumference, and absence of additional congenital anomalies.

2 | MATERIALS AND METHODS

We identified 15 individuals with de novo variants affecting codon 1740 in *SETD2*: 12 patients with c.5218C>T p.(Arg1740Trp) (Group 1) and 3 individuals with p c.5219G>A (Arg1740Gln) (Group 2). All patients were evaluated through clinical genetic services and ascertained retrospectively based on the presence of a missense variant affecting codon 1740 of *SETD2* through GeneDx, Ambry Genetics, GeneMatcher, Deciphering Developmental Disorders (DDD) and 100,000 Genomes Project (Firth et al., 2009; Sobreira, Schiettecatte, Valle, & Hamosh, 2015; The National Genomics Research and Healthcare Knowledgebase v5, 2019). Written consent was obtained for all patients for publication of their clinical phenotype, genotype, and photographs (where applicable). Detailed exome and genome testing methods are described in the supplemental material.

3 | RESULTS

3.1 | Clinical phenotype description

Group 1 consists of 12 individuals with the missense variant c.5218C>T p.(Arg1740Trp) in *SETD2* and strikingly similar features including: severe intellectual disability, seizures, microcephaly, cerebellar hypoplasia, hypoplasia of the corpus callosum, hypoplasia of the pons, Coats disease, similar facial features, and similar skeletal and internal organ anomalies. There are five male and seven female patients ranging from 1 month to 12 years of age at last clinical examination. Nine patients were born premature and four mothers of the premature babies had preeclampsia. Eight patients had normal head circumference at birth and two had microcephaly at birth (two female patients both with 31.5 cm head circumference at full term). Two patients' head circumference was unknown at birth. All patients with known length (seven patients) and known weight (12 patients) at birth were within the normal range. All patients in Group 1 had failure to thrive due to feeding difficulties and the majority required gastrostomy tube or nasogastric (NG) tube. The weight of patients in Group 1 remained below the 50th percentile through infancy and childhood (Table S1) in contrast to overgrowth and obesity described in LLS. The height was variable in Group 1 and all the recorded heights were within normal centiles (Table S1). Four patients' height was below the 10th centile, four patients' height was above the 75th centile, and one patient's height was at the 50th centile. The head circumference in Group 1 drifted below the third percentile in infancy in all patients. As the children became older, microcephaly was progressive and was at least 2.5 *SD* below the mean. Three patients' microcephaly progressed to greater than four standard deviations below the mean: Patient 3 is female and had head circumference of 34.5 cm at 3 months of age, Patient 7 is male and had head circumference of 37 cm at 5 months of age, and Patient 9 is female and had head circumference of 46 cm at 7 years of age. Additional common craniofacial features included hypertelorism, micrognathia, small upturned nose, biparietal narrowing, small forehead, flat face, short palpebral fissures, arched eyebrows, strabismus, broad nasal bridge and tip of the nose with low hanging columella, maxillary and mandibular hypoplasia, and slightly forward facing ears (Figure 1). Nine out of 12 patients had skeletal abnormalities of the hands and feet. Unique features of the appendicular skeleton included proximally implanted triphalangeal thumbs, broad proximally implanted halluces, hypoplastic distal phalanges and nails, and camptodactyly (Figure 2). Brain imaging by magnetic resonance imaging (MRI) or computed tomography (CT) scan revealed structural brain abnormalities in all individuals in Group 1. The abnormalities included hypoplasia of the corpus callosum, shallow sulci, ventriculomegaly, and large fluid filled space in the posterior fossa with ponto-cerebellar hypoplasia (Figures 3 and

FIGURE 1 Facial appearance with individuals from Group 1 (a) Patient 2 at 7 years old. (b, c) Patient 2 at 10 years old. (d, e) Patient 4 in infancy. (f, g) Patient 5 in infancy. (h, i) Patient 5 as a toddler. (j). Patient 6 as a toddler. (k) Patient 7 at 2 weeks old. (l) Patient 8 at 2 years-old. (m) Patient 8 at 12-years-old. (n,o) Patient 10 at 5 weeks old. Common facial features include hypertelorism, micrognathia, small upturned nose, biparietal narrowing, small forehead, microcephaly, flat face, short palpebral fissures, arched eyebrows, strabismus, broad nasal bridge, and tip of the nose with low hanging columella, maxillary and mandibular hypoplasia, and slightly forward facing ears

S1). None of the patients in Group 1 achieved speech or independent walking. Seven patients had seizures. All patients evaluated at greater than 2 months of age (10/12) developed ophthalmic abnormalities including telangiectasias of the retina with exudates (Coats disease like), retinal detachment, optic nerve coloboma and cataracts (Figure 4). Eight patients in Group 1 had mixed hearing loss. Eight of 12 patients had hyponatremia in infancy. Hyponatremia was initially concerning for syndrome of inappropriate antidiuretic hormone secretion (SIADH), but ultimately treated with sodium supplementation. Patient 6 in Group 1 also had acquired hypothyroidism and Patient 11 in Group 1 had a hypothalamic hamartoma. Eleven of 12 patients had urinary tract abnormalities including dilated collecting system and multicystic dysplastic kidneys. All five males in Group 1 had cryptorchidism and three had shawl scrotum. Two female patients had an anteriorly placed anus. Eleven of 12 patients also had congenital heart defects including ventricular septal defects, atrial septal defects, and aortic valve abnormalities. Ten of 12 patients had respiratory abnormalities beginning in their early infancy. The abnormalities included tracheomalacia, frequent aspiration, hypoventilation, desaturations, and sleep apnea. Three patients required tracheostomy and two required oxygen at night. Nine of 12 patients had skeletal abnormalities including hip dysplasia, contractures, thoracic dysplasia, and/or craniosynostosis. Patient 3 died at 1 month of age; he had hypoventilation and hypoplastic pulmonary arteries and veins. Detailed clinical information can be found in Table S1 and Figure S2.

Group 2 consists of three patients, two male and one female, with the missense variant c.5219G>A p.(Arg1740Gln) in *SETD2*. All three patients were born full term and prenatal findings in Patient 2 in Group 2 were significant for polyhydramnios. Growth measurements at birth for all individuals were within normal range. As the individuals got older, head circumference drifted to low normal, but never reached the criteria for microcephaly, while height was above the 50th percentile. All patients in Group 2 had speech delay but did achieve speech (Patient 2 in Group 2 was speaking in short sentences at 4 years 6 months), and two patients in this group also had mild motor developmental delay. Patient 2 in Group 2 had a normal brain

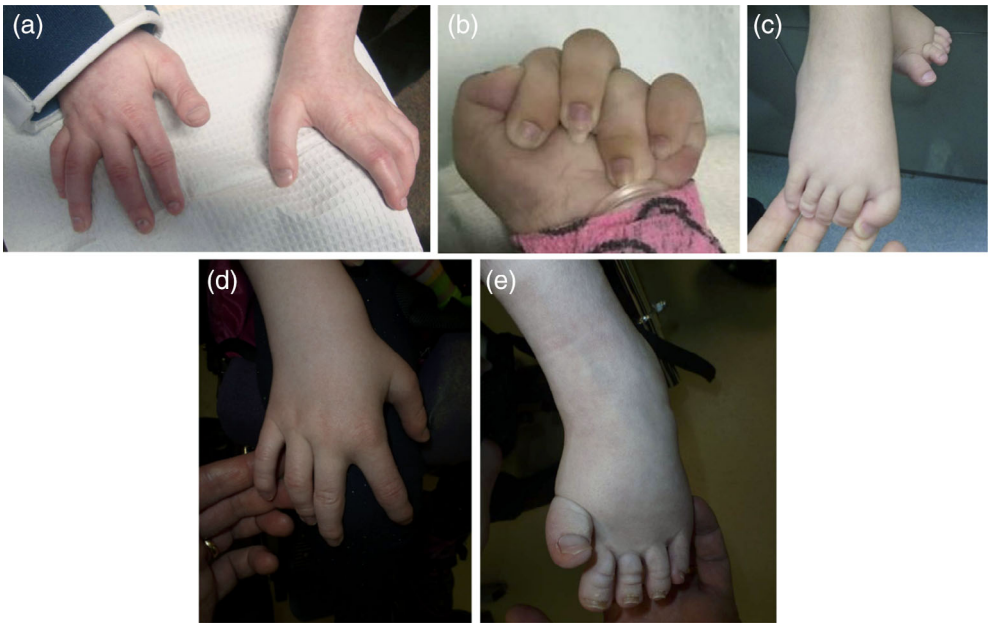

FIGURE 2 Images of the appendicular skeleton of individuals from Group 1. (a) Patient 2—Proximally implanted triphalangeal thumbs and camptodactyly. (b) Patient 4—Extreme camptodactyly with overlapping fingers and adducted thumb, hypoplastic distal phalanges, and nails. (c) Patient 5—Broad halluces and wide sandal gap. (d) Patient 8—Proximally implanted triphalangeal thumb and camtodactyly. (e) Patient 8—Broad proximally implanted hallux

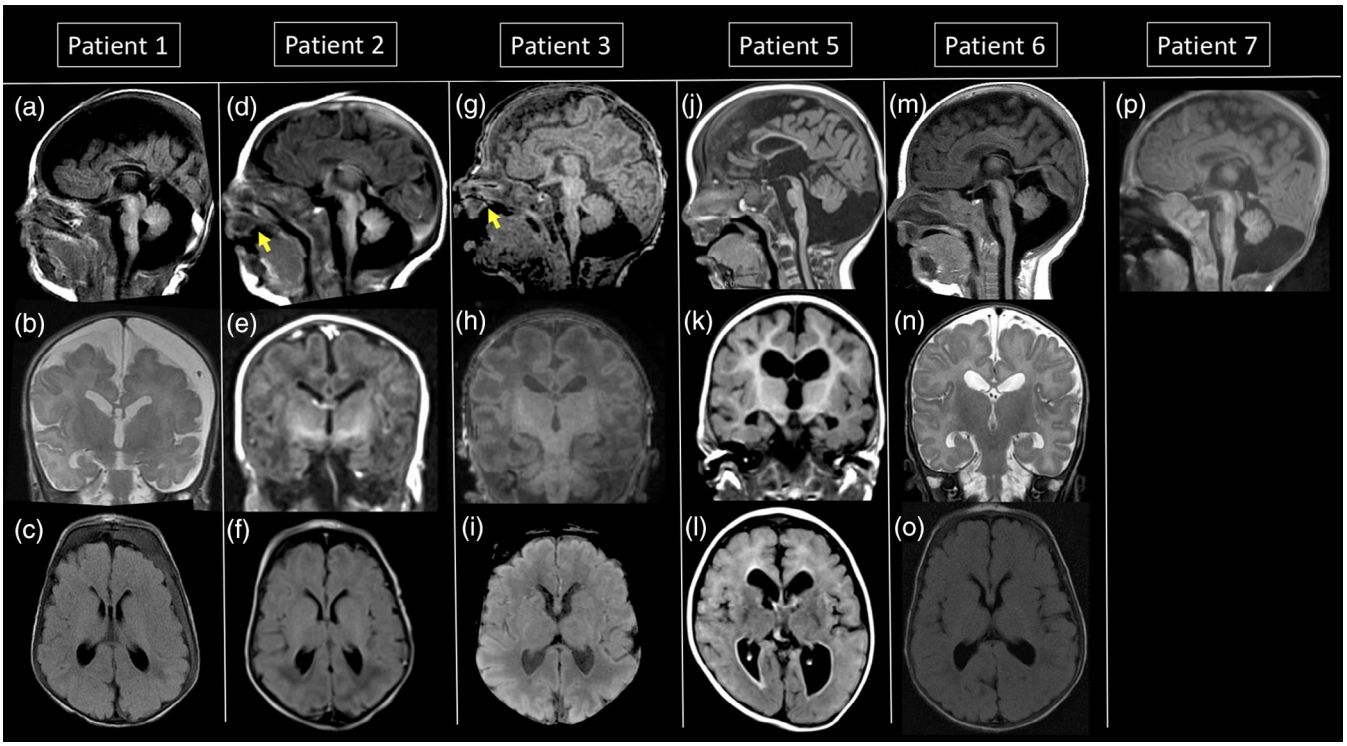

FIGURE 3 Magnetic resonance images of six patients with heterozygosity for a recurrent p.(Arg1740Trp) variant in *SETD2*, including sagittal T1-weighted images (a, d, g, j, m, p), Coronal T2- (b, n) and T1- (e, h, k) weighted images, and axial FLAIR images (c, f, i, l, o). Patients include a 6-week-old boy(Patient 1; a–c), a 4-day-old boy (Patient 2; d–f), a newborn girl (Patient 3; g–i), a 6-year-old girl (Patient 5; j–l), a 4-year-old boy (Patient 6; m–o), and a 2-month-old boy (Patient 7; o) . All patients have low craniofacial ratio (corresponding to clinical microcephaly), as well as a foreshortened and thin corpus callosum (a, d, g, j, m, p). Thinning of corpus callosum in a, d, g, and p could be due to a combination of callosal hypogenesis and unmyelinated state of white matter during the first few weeks of life. There is subtle overhanging appearance of the terminal portions of the frontal horns of lateral ventricles relative to the striatum (best seen on coronal b and e). Gyri are somewhat simplified and sulci are shallow (c, f, i, and l). All patients have cystic enlargement of the posterior fossa (mega cisterna magna) and prominent supracerebellar cisterns (a, d, g, and m). Slightly upturned hippocampi can be appreciated on coronal images (particularly in b, h, k, and n). Patient #1 has prominent convexity extra-axial spaces with left more than right subdural hemorrhage which may be related to birth trauma. A cleft palate can be seen in d and g (small arrows). Patient #5 has white matter volume loss (k, l), with enlargement of the third and lateral ventricles. Patient #5, #6, and #7 have probable persistent Blake pouch cyst (j, n, p). Patients #3, #5, and #6 (g, j, m) demonstrate abnormality of anteroposterior midbrain-hindbrain patterning (see text)

MRI. The oldest patient in Group 2 at last clinical evaluation was 15 years old and at that age, he achieved some reading and writing skills. Patient 3 in Group 2 had formal intelligence quotient (IQ) testing in childhood, which showed total IQ of 67, verbal IQ of 76, and performance IQ of 70. She had anxiety, executive functioning impairment, primarily fine motor developmental delay, and slow processing speed. None of the patients in Group 2 had any major medical issues. Patient 1 in Group 2 had constipation and laryngomalacia in infancy that resolved without intervention, Patient 2 in Group 2 had strabismus, normal hearing, and hypotonia, and Patient 3 in Group 2 had myopia and hypotonia. Facial features of Patient 1 in Group 2 included brachycephaly, upslanting palpebral fissures and straight upslanting eyebrows, and retrognathia (Figure 5). He also had slight fifth finger clinodactyly and camptodactyly. Patient 2 in Group 2 was not noted to have any dysmorphic facial features. He did have advanced bone age. Patient 3 in Group 2 was noted to have high arched palate, crowded teeth, retrognathia, and broad eyebrows. Detailed clinical information can be found in Table S1 and Figure S2.

4 | DISCUSSION

We describe 15 patients with variants at codon 1740 of *SETD2*. Twelve of the 15 patients (Group 1) present with a novel neurodevelopmental disorder that is associated with a tryptophan residue at codon 1740 of *SETD2*. These patients have common features and congenital anomalies suggestive of a novel syndrome. Patient 5 in Group 1 has been reported in the literature previously in a cohort of individuals with structural brain abnormalities (Aldinger et al., 2019). The c.5218C>T variant has an entry in ClinVar (VCV000388568.3) and is absent from population databases such as GnomAD (Karczewski et al., 2020; Landrum et al., 2017). The c.5218C>T variant is a nonconservative amino acid substitution. It is likely to impact

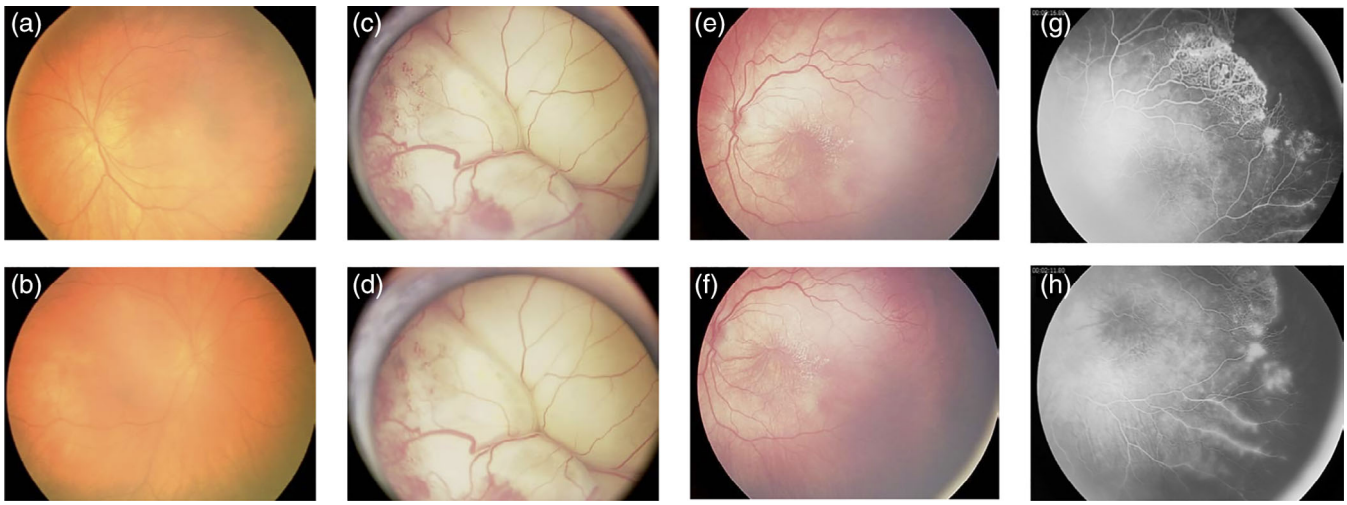

FIGURE 4 Ophthalmic images of Patient 8 in Group 1 (a) Left eye at 2 weeks of life: Blood vessels to far periphery of retina—normal (b) Right eye at 2 weeks of life: Normal (c, d) Right eye at 16 months old: Leukocoria, exudative detachment, and telangiectasia around periphery (e, f) Left eye at 16 months old in Fluorescein: blood vessels stop, and star exudate in macula (g) Left eye at 16 month old under prophylactic laser to avascular area and telangiectasia: Vessels stop, telangiectasia (h) Left eye at 16 months under despite laser localized to superior detachment: Avascular periphery and leakage of the dye

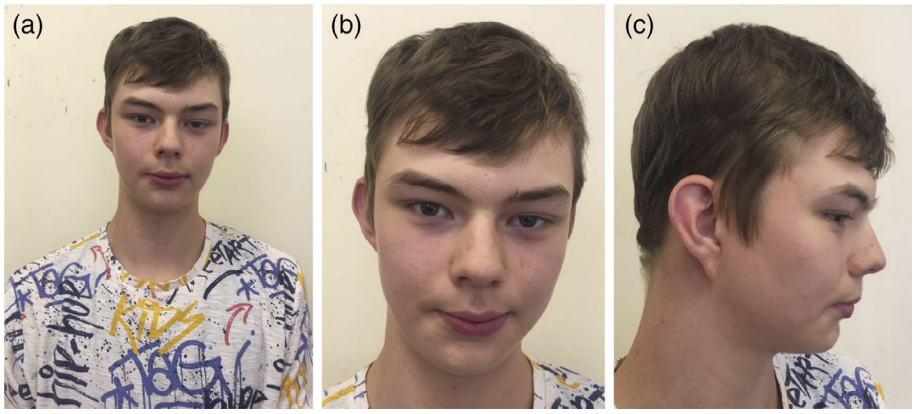

FIGURE 5 Facial appearance of Patient 2 in Group 2. (a–c). Patient at 15 years of age. Facial features include brachycephaly, upslanting palpebral fissures, and straight upslanting eyebrows

TABLE 1 Observed genotype–phenotype correlation of *SETD2* variants

Feature	Luscan Lumish syndrome (Lumish et al., 2015; Luscan et al., 2014; O'Roak, Vives, Fu, et al., 2012; O'Roak, Vives, Girirajan, et al., 2012; Tlemsani et al., 2016; van Rij et al., 2018)	Cases with c.5218C > T p.(Arg1740Trp) (Group 1 reported in this article)	Cases p.R1740Q c.5219G > A p.(Arg1740Gln) (Group 2 reported in this article)
Inheritance	Autosomal dominant	Autosomal dominant, all de novo	Autosomal dominant, all de novo
Growth			
Failure to thrive in infancy HP:0001531	0/10 (0%)	12/12 (100%)	0/3 (0%)
Overgrowth HP.0001548 and/or Obesity HP.0001513	9/9 (100%)	0/12 (0%)	0/3 (0%)
Neurodevelopment			
Intellectual disability HP:0001249/global Developmental delay HP:0001263	7/9 (78%)	12/12 (100%)	3/3 (100%)
Autism HP.0000717	7/7 (100%)	0/12 (0%)	0/3 (0%)
Seizures HP:0001250	1/6 (17%)	7/12 (58%)	0/3 (0%)
Hypotonia HP:0001290	0/7 (0%)	12/12 (100%)	2/3 (67%)
Craniofacial			
Macrocephaly, postnatal HP.0000256	8/8 (100%)	0/12 (0%)	0/3 (0%)
Microcephaly HP.0000252	0/8 (0%)	12/12 (100%)	0/3 (0%)
Long face HP.0000276	3/5 (60%)	0/12 (0%)	0/3 (0%)
Broad nasal tip HP:0000455	0/5 (0%)	9/12 (75%)	1/3 (33%)
Low hanging Columella HP:0009765	0/5 (0%)	9/12 (75%)	0/3 (0%)
Wide nasal bridge HP:0000431	1/5 (20%)	9/12 (75%)	0/3 (0%)
Hypoplasia of the Maxilla HP:0000327/ Midface Retrusion HP:0011800	0/5 (0%)	8/12 (67%)	0/3 (0%)
Malar flattening HP:0000272	1/5 (20%)	0/12 (0%)	1/3 (33%)
Large mandible HP.0000303	3/5 (60%)	0/12 (0%)	0/3 (0%)
Pointed chin HP.0000307	3/5 (60%)	0/12 (0%)	1/3 (33%)
Hypertelorism HP.0000316	2/5 (40%)	12/12 (100%)	0/3 (0%)
Short palpebral fissures HP.0012745	0/5 (0%)	8/12 (67%)	0/3 (0%)
Downslanted palpebral fissures HP.0000494	2/5 (40%)	0/7 (0%)	0/3 (0%)
Upslanted palpebral fissures HP.0000582	0/5 (0%)	5/7 (71%)	1/3 (33%)
Highly arched Eyebrow HP:0002553	0/5 (0%)	11/12 (92%)	0/3 (0%)
Periorbital fullness HP.0000629	0/5 (0%)	8/12 (67%)	0/3 (0%)
Micrognathia HP.0000347	0/5 (0%)	12/12 (100%)	0/3 (0%)
Retrognathia HP:0000278	0/5 (0%)	0/12 (0%)	2/3 (67%)

(Continues)

TABLE 1 (Continued)

Feature	Luscan Lumish syndrome (Lumish et al., 2015; Luscan et al., 2014; O'Roak, Vives, Fu, et al., 2012; O'Roak, Vives, Girirajan, et al., 2012; Tlemsani et al., 2016; van Rij et al., 2018)	Cases with c.5218C > T p.(Arg1740Trp) (Group 1 reported in this article)	Cases p.R1740Q c.5219G > A p.(Arg1740Gln) (Group 2 reported in this article)
Brain malformations			
Hydrocephalus HP.0000238	1/10 (10%)	0/12 (0%)	0/3 (0%)
Chiari type 1 HP.0007099	1/10 (10%)	0/12 (0%)	0/3 (0%)
Hypoplasia of corpus Callosum HP.0002079	0/10 (0%)	9/12 (100%)	0/3 (0%)
Hypoplasia of The pons HP:0012110	0/10 (0%)	8/12(100%)	0/3 (0%)
Cerebellar hypoplasia HP.0001321	0/10 (0%)	12/12 (100%)	0/3 (0%)
Eye abnormalities			
Retinal telangiectasia HP.0007763	0/10 (0%)	8/10 (80%)	0/3 (0%)
Optic nerve hypoplasia HP:0000609	0/10 (0%)	3/10 (30%)	0/3 (0%)
Retinal detachment HP:0000541	0/10 (0%)	5/10 (50%)	0/3 (0%)
Cataract HP:0000518	0/10 (0%)	2/10 (20%)	0/3 (0%)
Hearing loss			
Sensorineural HP:0000407	0/10 (0%)	6/8 (75%)	0/3 (0%)
Conductive HP:0000405	0/10 (0%)	7/8 (88%)	0/3 (0%)
Respiratory			
Hypoventilation HP:0002791	0/10 (0%)	9/12 (75%)	0/3 (0%)
Tracheomalacia HP:0002779	0/10 (0%)	2/12 (17%)	0/3 (0%)
Gastrointestinal			
Feeding difficulties HP:0011968	0/10 (0%)	12/12 (100%)	0/3 (0%)
Endocrine			
Hyponatremia HP:0002902	0/10 (0%)	8/12 (67%)	0/3 (0%)
Congenital heart defect HP:0001627	0/10 (0%)	11/12 (92%)	0/3 (0%)
Skeletal abnormalities HP:0000924	5/6 (83%)	12/12 (100%)	2/3 (67%)
Genitourinary tract anomalies HP:0000119	0/7 (0%)	11/12 (92%)	0/3 (0%)

secondary protein structure because the arginine and tryptophan residues differ in polarity, charge, and size. In silico analyses that included protein predictors and evolutionary conservation supported a deleterious effect (Schwarz, Cooper, Schuelke, & Seelow, 2014). Three out of 15 patients (Group 2) have residue glutamine at codon 1740 of *SETD2*. The c.5219G>A variant is absent from population databases such as GnomAD and is predicted deleterious according to in silico analyses (Karczewski et al., 2020; Landrum et al., 2017; Schwarz et al., 2014). The patients in Group 2 appear to have a different neurodevelopmental phenotype than Group 1 and absence of major malformations. Individuals with variants in other codons of *SETD2* have a neurodevelopmental disorder known as LLS that includes macrocephaly, overgrowth or obesity, large pointed mandible, autism, and normal to moderate intellectual disabilities without congenital malformations of internal organs. It appears that the p.(Arg1740Trp) and p.(Arg1740Gln) mutations in *SETD2* have clear genotype–phenotype correlation displaying clinical features distinct from each other and from individuals with other mutations in *SETD2* (Table 1). The presentation of individuals in Group 1 is strikingly similar and includes rare and unique disorders, such as Coats disease (MIM# 300216) with no clearly established molecular etiology. The intellectual disability of individuals in Group 2 with p.(Arg1740Gln) is more

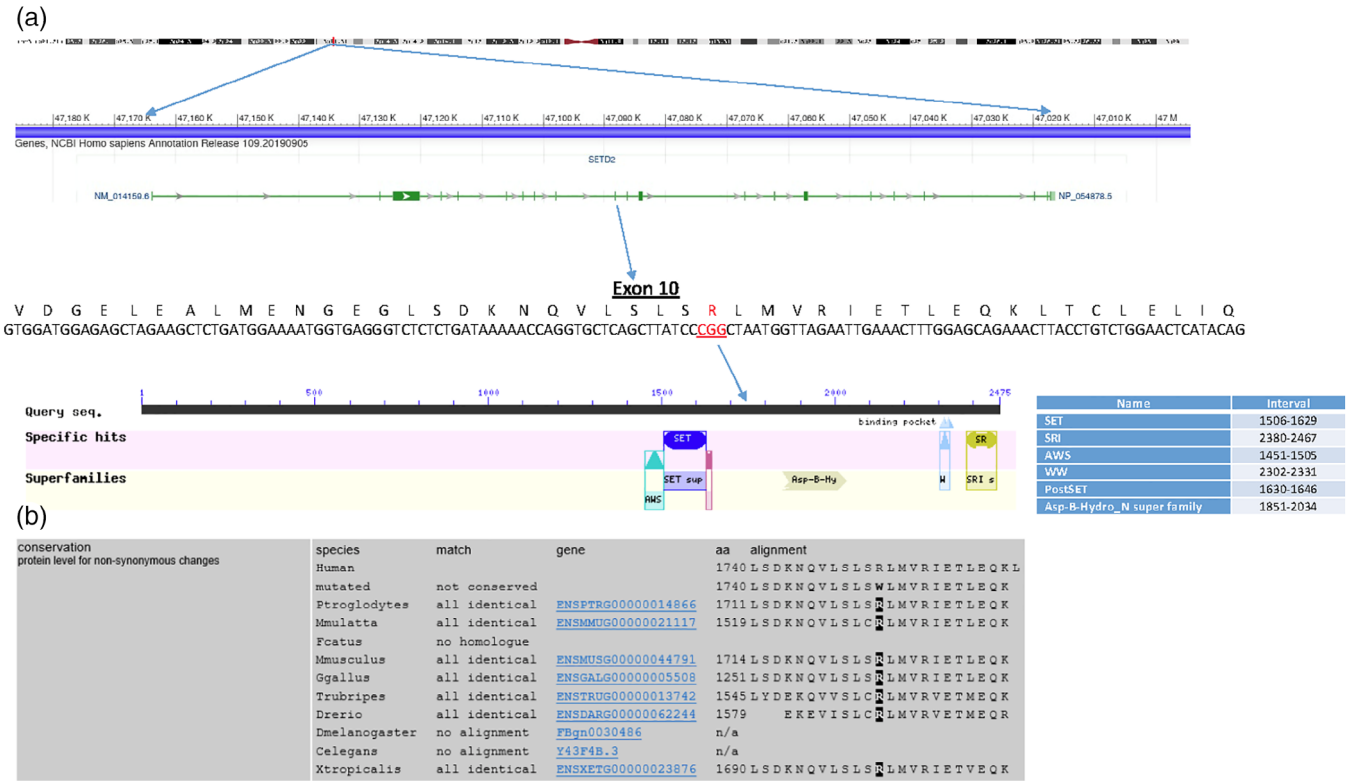

Name	Interval
SET	1506-1629
SRI	2380-2467
AWS	1451-1505
WW	2302-2331
PostSET	1630-1646
Asp-B-Hydro_N super family	1851-2034

FIGURE 6 Molecular coordinates and conservation of SETD2. (a) The genomic coordinates of *SETD2* at 3p21.31 (UCSC browser GRCh38/hg38 assembly). The isoform 1 of *SETD2* depicting exons and introns. The NM_014189.6 sequence of exon 10 and the position of codon 1740 in the protein depicted with conserved domains (https://www.ncbi.nlm.nih.gov/Structure/cdd/wrpsb.cgi?seqinput=XP_024309255.1). (b) Conservation of the arginine at 1740 of SETD2 across multiple species (Schwarz et al., 2014)

severe than individuals other *SETD2* mutations, but not as severe as individuals in Group 1 with p.(Arg1740Trp). Individuals in Group 2 lack major medical malformations, which is similar to individuals with LLS. Abnormal neurodevelopment in patients with LLS and patients described here suggest that normal function of *SETD2* is important for neurological development. More specifically, codon 1740 appears to be critically important for normal *SETD2* function, due to the profound clinical abnormalities seen in patients with a mutation at this site.

The SETD2 protein contains three functional domains that are evolutionarily conserved: AWS-SET-PostSET domain, WW domain, and SRI domain (Figure 6). The protein also comprises a coiled coil motif and low charged region (Hacker et al., 2016; Sun et al., 2005). The SET domain is responsible for transferring methyl groups, the WW domain facilitates protein–protein interactions, and the SRI domain interacts with RNA polymerase II, specifically the hyperphosphorylated C-terminal domain of the Rpb1 subunit (Li et al., 2016; Xie et al., 2008). The SRI domain directs SETD2 activity toward genes that are actively transcribed. The SETD2 protein has been shown to interact with many downstream pathways and plays an important role in epigenetic regulation (Greer & Shi, 2012; Terzo et al., 2019; Xie et al., 2008).

The variants described here are downstream of the SET domain, but upstream of the coiled coil motif (Figure 6) (Marchler-Bauer et al., 2016). Codon 1740 is not included in a domain or site with known specific function and it is not included in a known unique region of the protein (UniPortKB - Q9BYW2, RCSB PDB) (UniProt Consortium, 2018). It remains to be determined which of the SETD2-dependent cellular mechanisms are compromised by variants affecting codon 1740. This codon is caudal from the catalytic SET methyltransferase domain mapped to amino acids 1,550–1,667 of the protein (Hacker et al., 2016). We note that codon 1740 is in close proximity to the p.Asn1734Asp and p.Ser1769Asp substitutions that are, in the affected cancer cell lines, associated with near-complete loss of SETD2 protein by immunoblot (Li et al., 2013). However, it is unclear how the p.(Arg1740Trp) and p.(Arg1740Gln) mutations alter protein activity. The reasons for the reduction in tissue/cell protein level of the p.Asn1734Asp and p.Ser1769Asp substitutions is currently unknown. In the Cosmic database, the c.5218C > T p.(Arg1740Trp) variant was recorded four times in a variety of tumors (Tate et al., 2018). Codon 1740 is downstream of the region that includes codons 1418–1714 of SETD2; this region is suggested as the domain that interacts with TUBA1A (Park et al., 2016).

There is some laboratory evidence that deficiency of *SETD2* is associated with loss of H3K36me3 and failure to establish the correct DNA methylome (Xu et al., 2019). Hypomethylation of histone H3 at K36 (H3K36me2) because of haploinsufficiency of *NSD1* is associated with overgrowth in Sotos syndrome (MIM# 117550). Hypomethylation of intergenic DNA because of haploinsufficiency of *DNMT3A* is

associated with overgrowth in Tatton-Brown-Rahman syndrome (MIM# 615879) (Weinberg et al., 2019). The PWWP domain of DNMT3A has binding affinity with both H3K36me2 and H3K36me3 and genetic ablation of *Nsd1* and its paralogue *Nsd2* in mice cells results in redistribution of DNMT3A from H3K36me2 to H3K36me3 and aberrant intergenic CpG methylation (Weinberg et al., 2019). Disruption of *Setd2* in the same mice cells with genetic ablation of *Nsd1* and its paralogue *Nsd2* impaired localization of *DNMT3A* to gene bodies resulting in aberrant intergenic methylation as seen in overgrowth syndromes and cancer (Weinberg et al., 2019). It is likely that loss of function variants in *SETD2* are associated with overgrowth similarly to loss of function in *NSD1* and *DNMT3A*, as seen with LLS. The p.(Arg1740Trp) mutation in *SETD2* is associated with a severe neurodevelopmental syndrome and microcephaly and the p.(Arg1740Gln) mutation is associated with a neurodevelopmental phenotype and low normal head circumference. Neither of these variants are associated with overgrowth. Recently, gain-of-function mutations in *DNMT3A* have been associated with microcephalic dwarfism and hypermethylation of Polycomb-regulated regions (Heyn et al., 2019). It is possible that the two variants affecting codon 1740 of *SETD2* have a similar affect to the gain-of-function variants of *DMNT3A*. It is possible that these variants are gain-of-function, have effects on epigenetic regulation, or affect posttranslational modification of the cytoskeleton; however, future studies are needed to elucidate the pathogenic mechanism of variants affecting codon 1740 of *SETD2*. Whole genome methylation analysis of available cell lines in our cohorts and individuals with LLS may provide insight to possible differences on epigenetic regulation of *SETD2* variants. Expression of the SETD2 protein is ubiquitous; therefore, studying levels of the protein in peripheral blood and accessible tissues of our cohorts, as well as HEK 293 cell lines expressing different variants, may provide information about cellular function of *SETD2* variants.

5 | CONCLUSION

We describe the genotype–phenotype correlations of variants affecting codon 1740 of *SETD2* in comparison to other pathogenic variants in this gene. The two groups of patients presented here reveal a novel spectrum of phenotypic heterogeneity associated with *SETD2*. The recurrent c.5218C>T p.(Arg1740Trp) variant in the *SETD2* gene appears to be associated with a novel severe neurodevelopmental disorder with multiple congenital anomalies involving several organ systems. Individuals who are heterozygous for this variant (Group 1) have strikingly similar features that include microcephaly, intellectual disability, seizures, congenital heart defects, congenital brain abnormalities, congenital urogenital abnormalities, ophthalmic abnormalities, hyponatremia in infancy, feeding difficulties, and facial dysmorphia. These phenotypic characteristics appear to be specific to tryptophan at codon 1740, as individuals with this variant appear to have a different syndrome from the previously described LLS and different from the individuals that we describe with a glutamine at codon 1740 (Group 2). Individuals in Group 2 have a distinctive neurodevelopmental disorder with low normal head circumference, moderate to severe intellectual disability, and absence of congenital anomalies. The syndromes described in Groups 1 and 2 are novel and the syndrome described in Group 1 presents with a recognizable pattern of congenital malformations and dysmorphic features (Table 1). Further research is required to delineate the pathogenesis of variants associated with codon 1740 to better understand their phenotypic consequences.

ACKNOWLEDGMENTS

We would like to thank the patients and their families. This research was made possible through access to the data and findings generated by the 100,000 Genomes Project. The 100,000 Genomes Project is managed by Genomics England Limited (a wholly owned company of the Department of Health and Social Care). The 100,000 Genomes Project is funded by the National Institute for Health Research and NHS England. The Wellcome Trust, Cancer Research UK and the Medical Research Council have also funded research infrastructure. The 100,000 Genomes Project uses data provided by patients and collected by the National Health Service as part of their care and support. The DDD study presents independent research commissioned by the Health Innovation Challenge Fund [grant number HICF-1009-003], a parallel funding partnership between Wellcome and the Department of Health, and the Wellcome Sanger Institute [grant number WT098051]. The views expressed in this publication are those of the author(s) and not necessarily those of Wellcome or the Department of Health. The study has UK Research Ethics Committee approval (10/H0305/83, granted by the Cambridge South REC, and GEN/284/12 granted by the Republic of Ireland REC). The research team acknowledges the support of the National Institute for Health Research, through the Comprehensive Clinical Research Network.

This work was supported by the DFG grant PO2366/2-1 to B. P.

CONFLICT OF INTEREST

K. Mc., J. K. R., S. P., and I. M. W. are employees of GeneDx, Inc. K. R. is a Full-time salaried employee of Ambry genetics.

AUTHOR CONTRIBUTATIONS

Rachel Rabin: Patient cohort information management. All others (Alireza Radmanesh; Ian A. Glass; William B. Dobyns; Kimberly A. Aldinger; Joseph T. Shieh; Shelby Romoser; Hannah Bombei; Leah Dowsett; Pamela Trapane; John A. Bernat; Janice Baker; Nancy J. Mendelsohn; Bernt Popp; Manuela Siekmeyer; Ina Sorge; Francis Hugh Sansbury; Patrick Watts; Nicola C. Foulds; Jennifer Burton; George Hoganson; Jane A. Hurst; Lara Menzies; Deborah Osio; Larissa Kerecuk; Jan M. Cobben; Khadijé Jizi; Sebastien Jacquemont; Stacey A. Bélanger; Katharina Löhner; Hermine E. Veenstra-Knol; Henny H. Lemmink; Jennifer Keller-Ramey; Ingrid M. Wentzensen; Sumit Punj; Kirsty McWalter; Jerica Lenberg; Katarzyna A. Ellsworth; Kelly Radtke; Schahram Akbarian)provided clinical information about cases and critical reviews of the initial manuscripts.

DATA AVAILABILITY STATEMENT

The data that support the findings of this study are openly available in the supplementary material of this article.

ORCID

Rachel Rabin https://orcid.org/0000-0003-4906-7428
William B. Dobyns https://orcid.org/0000-0002-7681-2844
Leah Dowsett https://orcid.org/0000-0002-8095-9793
Schahram Akbarian https://orcid.org/0000-0001-7700-0891
John Pappas https://orcid.org/0000-0001-5625-2598

REFERENCES

Aldinger, K. A., Timms, A. E., Thomson, Z., Mirzaa, G. M., Bennett, J. T., Rosenberg, A. B., … Cheng, C. V. (2019). Redefining the etiologic landscape of cerebellar malformations. *The American Journal of Human Genetics*, *105*(3), 606–615.

Chen, K., Liu, J., Liu, S., Xia, M., Zhang, X., Han, D., … Cao, X. (2017). Methyltransferase SETD2-mediated methylation of STAT1 is critical for interferon antiviral activity. *Cell*, *170*(3), 492–506.

Edmunds, J. W., Mahadevan, L. C., & Clayton, A. L. (2008). Dynamic histone H3 methylation during gene induction: HYPB/Setd2 mediates all H3K36 trimethylation. *The EMBO Journal*, *27*(2), 406–420.

Firth, H. V., Richards, S. M., Bevan, A. P., Clayton, S., Corpas, M., Rajan, D., … Carter, N. P. (2009). DECIPHER: Database of chromosomal imbalance and phenotype in humans using ensembl resources. *The American Journal of Human Genetics*, *84*(4), 524–533.

Greer, E. L., & Shi, Y. (2012). Histone methylation: A dynamic mark in health, disease and inheritance. *Nature Reviews Genetics*, *13*(5), 343–357.

Hacker, K. E., Fahey, C. C., Shinsky, S. A., Chiang, Y. C. J., DiFiore, J. V., Jha, D. K., … Rathmell, W. K. (2016). Structure/function analysis of recurrent mutations in SETD2 protein reveals a critical and conserved role for a SET domain residue in maintaining protein stability and histone H3 Lys-36 trimethylation. *Journal of Biological Chemistry*, *291*(40), 21283–21295.

Heyn, P., Logan, C. V., Fluteau, A., Challis, R. C., Auchynnikava, T., Martin, C. A., … Cormier-Daire, V. (2019). Gain-of-function DNMT3A mutations cause microcephalic dwarfism and hypermethylation of Polycomb-regulated regions. *Nature Genetics*, *51*(1), 96–105.

Hu, M., Sun, X. J., Zhang, Y. L., Kuang, Y., Hu, C. Q., Wu, W. L., … Xiao, H. S. (2010). Histone H3 lysine 36 methyltransferase Hypb/Setd2 is required for embryonic vascular remodeling. *Proceedings of the National Academy of Sciences*, *107*(7), 2956–2961.

Iossifov, I., O'roak, B. J., Sanders, S. J., Ronemus, M., Krumm, N., Levy, D., … Smith, J. D. (2014). The contribution of de novo coding mutations to autism spectrum disorder. *Nature*, *515*(7526), 216–221.

Karczewski, K. J., Francioli, L. C., Tiao, G., Cummings, B. B., Alföldi, J., Wang, Q., … Gauthier, L. D. (2020). The mutational constraint spectrum quantified from variation in 141,456 humans. *Nature*, *581*(7809), 434–443. https://doi.org/10.1038/s41586-020-2308-7.

Landrum, M. J., Lee, J. M., Benson, M., Brown, G. R., Chao, C., Chitipiralla, S., … Karapetyan, K. (2017). ClinVar: Improving access to variant interpretations and supporting evidence. *Nucleic Acids Research*, *46*(D1), D1062–D1067.

Lek, M., Karczewski, K. J., Minikel, E. V., Samocha, K. E., Banks, E., Fennell, T., … Tukiainen, T. (2016). Analysis of protein-coding genetic variation in 60,706 humans. *Nature*, *536*(7616), 285–291.

Li, F., Mao, G., Tong, D., Huang, J., Gu, L., Yang, W., & Li, G. M. (2013). The histone mark H3K36me3 regulates human DNA mismatch repair through its interaction with MutSα. *Cell*, *153*(3), 590–600.

Li, J., Duns, G., Westers, H., Sijmons, R., van den Berg, A., & Kok, K. (2016). SETD2: An epigenetic modifier with tumor suppressor functionality. *Oncotarget*, *7*(31), 50719–50734.

Lumish, H. S., Wynn, J., Devinsky, O., & Chung, W. K. (2015). Brief report: SETD2 mutation in a child with autism, intellectual disabilities and epilepsy. *Journal of Autism and Developmental Disorders*, *45*(11), 3764–3770.

Luscan, A., Laurendeau, I., Malan, V., Francannet, C., Odent, S., Giuliano, F., … Cormier-Daire, V. (2014). Mutations in SETD2 cause a novel overgrowth condition. *Journal of Medical Genetics*, *51*(8), 512–517.

Marchler-Bauer, A., Bo, Y., Han, L., He, J., Lanczycki, C. J., Lu, S., … Gwadz, M. (2016). CDD/SPARCLE: Functional classification of proteins via subfamily domain architectures. *Nucleic Acids Research*, *45* (D1), D200–D203.

McDaniel, S. L., & Strahl, B. D. (2017). Shaping the cellular landscape with Set2/SETD2 methylation. *Cellular and Molecular Life Sciences*, *74*(18), 3317–3334.

O'Roak, B. J., Vives, L., Fu, W., Egertson, J. D., Stanaway, I. B., Phelps, I. G., … Munson, J. (2012). Multiplex targeted sequencing identifies recurrently mutated genes in autism spectrum disorders. *Science*, *338* (6114), 1619–1622.

O'Roak, B. J., Vives, L., Girirajan, S., Karakoc, E., Krumm, N., Coe, B. P., … Turner, E. H. (2012). Sporadic autism exomes reveal a highly interconnected protein network of de novo mutations. *Nature*, *485*(7397), 246–250.

Park, I. Y., Powell, R. T., Tripathi, D. N., Dere, R., Ho, T. H., Blasius, T. L., … Verhey, K. J. (2016). Dual chromatin and cytoskeletal remodeling by SETD2. *Cell*, *166*(4), 950–962.

Rega, S., Stiewe, T., Chang, D. I., Pollmeier, B., Esche, H., Bardenheuer, W., … Pützer, B. M. (2001). Identification of the full-length huntingtin-interacting protein p231HBP/HYPB as a DNA-binding factor. *Molecular and Cellular Neuroscience*, *18*(1), 68–79.

Schwarz, J. M., Cooper, D. N., Schuelke, M., & Seelow, D. (2014). MutationTaster2: Mutation prediction for the deep-sequencing age. *Nature Methods*, *11*(4), 361–362.

Sobreira, N., Schiettecatte, F., Valle, D., & Hamosh, A. (2015). GeneMatcher: A matching tool for connecting investigators with an interest in the same gene. *Human Mutation*, *36*(10), 928–930.

Sun, X. J., Wei, J., Wu, X. Y., Hu, M., Wang, L., Wang, H. H., … Chen, Z. (2005). Identification and characterization of a novel human histone H3 lysine 36-specific methyltransferase. *Journal of Biological Chemistry*, *280*(42), 35261–35271.

Tate, J. G., Bamford, S., Jubb, H. C., Sondka, Z., Beare, D. M., Bindal, N., … Fish, P. (2018). COSMIC: The catalogue of somatic mutations in cancer. *Nucleic Acids Research*, *47*(D1), D941–D947.

Terzo, E. A., Lim, A. R., Chytil, A., Chiang, Y. C., Farmer, L., Gessner, K. H., … Rathmell, W. K. (2019). SETD2 loss sensitizes cells to PI3Kβ and AKT inhibition. *Oncotarget*, *10*(6), 647–659.

The National Genomics Research and Healthcare Knowledgebase v5 (2019). Genomics England. doi:https://doi.org/10.6084/m9.figshare.4530893.v5.

Tlemsani, C., Luscan, A., Leulliot, N., Bieth, E., Afenjar, A., Baujat, G., … Odent, S. (2016). SETD2 and DNMT3A screen in the Sotos-like syndrome French cohort. *Journal of Medical Genetics*, *53*(11), 743–751.

UniProt Consortium. (2018). UniProt: A worldwide hub of protein knowledge. *Nucleic Acids Research*, *47*(D1), D506–D515.

van Rij, M. C., Hollink, I. H., Terhal, P. A., Kant, S. G., Ruivenkamp, C., van Haeringen, A., … van Belzen, M. J. (2018). Two novel cases expanding the phenotype of SETD2-related overgrowth syndrome. *American Journal of Medical Genetics Part A*, *176*(5), 1212–1215.

Weinberg, D. N., Papillon-Cavanagh, S., Chen, H., Yue, Y., Chen, X., Rajagopalan, K. N., … Lemiesz, A. E. (2019). The histone mark

H3K36me2 recruits DNMT3A and shapes the intergenic DNA methylation landscape. *Nature*, *573*(7773), 281–286.

Xie, P., Tian, C., An, L., Nie, J., Lu, K., Xing, G., … He, F. (2008). Histone methyltransferase protein SETD2 interacts with p53 and selectively regulates its downstream genes. *Cellular Signalling*, *20*(9), 1671–1678.

Xu, Q., Xiang, Y., Wang, Q., Wang, L., Brind'Amour, J., Bogutz, A. B., … Du, Z. (2019). SETD2 regulates the maternal epigenome, genomic imprinting and embryonic development. *Nature Genetics*, *51*(5), 844–856.

Zhou, V. W., Goren, A., & Bernstein, B. E. (2011). Charting histone modifications and the functional organization of mammalian genomes. *Nature Reviews Genetics*, *12*(1), 7–18.

SUPPORTING INFORMATION

Additional supporting information may be found online in the Supporting Information section at the end of this article.

How to cite this article: Rabin R, Radmanesh A, Glass IA, et al. Genotype–phenotype correlation at codon 1740 of *SETD2*. *Am J Med Genet Part A*. 2020;182A:2037–2048. https://doi.org/10.1002/ajmg.a.61724